Proc. Natl. Acad. Sci. USA
Vol. 82, pp. 6889–6893, October 1985
Cell Biology

Microtubule distribution in cultured cells and intact tissues: Improved immunolabeling resolution through the use of reversible embedment cytochemistry

(immunocytochemistry/post-embedding labeling/polymethylmethacrylate/immunofluorescence/high-voltage electron microscopy)

GARY GORBSKY* AND GARY G. BORISY

High-Voltage Electron Microscope Facility and Laboratory of Molecular Biology, University of Wisconsin, Madison, WI 53706

Communicated by Hans Ris, June 14, 1985

ABSTRACT **To investigate the detailed distributions of microtubules in cultured cells and intact tissues we developed a reversible embedment method for antibody labeling of sectioned material. Fixed tissues were infiltrated with fully polymerized polymethylmethacrylate dissolved in an organic solvent. Evaporation of the solvent left the tissue embedded in hard plastic. After sectioning by conventional methods, the plastic was extracted and sections were processed for indirect immunofluorescence to label microtubules. Clear images of microtubules were observed in sections of cultured epithelial cells, intact chick intestinal epithelium, and dividing sea urchin eggs. Microtubules in the differentiated epithelium of the chick intestine generally paralleled the long axis of the cells and did not focus on a microtubule-organizing center. Mitotic cells of the intestinal epithelium appeared similar to the mitotic cells of epithelial lines in culture. In sections of dividing sea urchin eggs detailed images of spindle and astral fibers were revealed. Immunoelectron microscopic labeling for tubulin was performed on sections of Pt K1 cells using secondary antibodies adsorbed to 20-nm gold particles. Semi-thick sections viewed by high-voltage electron microscopy showed both the overall distribution of microtubules and their detailed interactions with other cellular organelles. Mitochondria were often aligned along labeled microtubules. Reversible embedment cytochemistry should provide a general method for high resolution labeling of cells and tissues with affinity probes.**

The distribution of cellular microtubules is conveniently revealed through the use of antibodies coupled to markers that can be visualized by light or electron microscopy. In whole mount immunofluorescence of cells grown on coverslips, individual microtubules are ordinarily resolved only in thin cellular processes. Often these same cells round up in mitosis, further obscuring the pattern of individual microtubules. The resolution in thicker regions of cultured cells can be improved by labeling cells, embedding them in plastic, and cutting sections <1 μm (1). For intact tissues, where the penetration of antibody probes is more limited, postembedding labeling of sectioned material is more common. However, the paraffin or cryostat sections used in classical immunocytochemistry are simply too thick (>2 μm) to allow clear observation of single microtubules.

At the electron microscopic level, the conflicting demands of probe visibility and specimen contrast and of antigen accessibility and structural preservation render many immunolabeling techniques laborious and/or unreliable. Even peroxidase, a small marker, often shows only limited penetration into intact pieces of tissue (2). Special tissue permeabilization treatments can aid the penetration of immunological reagents (3–5), but the larger probes (e.g., ferritin and very small gold particles) penetrate even more poorly and give limited contrast, making visualization possible only at very high magnifications. Tracing the extended arrays of cytoskeletal elements is also limited by the necessity to observe thin sections which contain only a small fraction of the microtubules present in a cell.

One approach toward minimizing the problem of antigen accessibility has been to develop post-embedding methods for high-resolution immunoelectron microscopy. Commonly, antibodies coupled to electron-dense markers are applied to thin sections of samples embedded in Epon (6–10) or various acrylic plastics (11–18). However, since the plastic remains during labeling, antibodies apparently bind only to those antigens exposed at surfaces of the section (19). Although useful for labeling antigens in membranes or vesicles, such techniques are generally inappropriate for cytoskeletal elements since these filaments are very thin and tend to lie within the section.

This limitation has been partially overcome for light and electron microscopic immunolabeling through the use of reversible embedding procedures, in which the embedment is removed after cutting semi-thick (<1.0 μm) or thin sections. Most commonly, tissues are supported for sectioning or fracturing by embedment in ice (20–26) or in a hard wax such as polyethylene glycol (PEG) (27, 28). Subsequently, the embedding medium is removed and antibodies are applied. Parysek *et al.* (29) using PEG embedding, recently produced immunofluorescent images apparently showing individual microtubules in semithick sections of mouse tissues. However, ultracryotomy and wax embedding have certain limitations. Specialized equipment is necessary for ultracryotomy. Both ice and PEG embedments require nonstandard sectioning procedures that preclude, for all practical purposes, the production of long ribbons of serial sections or sections of tissue culture cells cut parallel to the substratum. Moreover, the ultrastructural preservation obtained by these procedures has appeared generally inferior to that seen in conventional epoxy sections.

We present here an examination of microtubule arrays in sections of tissue culture cells and intact tissues using an embedding technique that we have named reversible embedment cytochemistry (REC). The advantages of this method include maximization of antigenicity by embedment of tissues in plastic without exposure to polymerization reactions and the simplification of sectioning procedures. Intense immunofluorescent labeling of microtubules was obtained in sections of cultured cells cut parallel to their substratum, in sections of chick intestinal epithelium, and in sections of a

The publication costs of this article were defrayed in part by page charge payment. This article must therefore be hereby marked "*advertisement*" in accordance with 18 U.S.C. §1734 solely to indicate this fact.

Abbreviations: MTOC, microtubule-organizing center; REC, reversible embedment cytochemistry.

*To whom reprint requests should be addressed at: Laboratory of Molecular Biology, University of Wisconsin, 1525 Linden Drive, Madison, WI 53706.

very large cell—a mitotic sea urchin egg. Finally, in sections of cultured cells immunolabeled using colloidal gold, we observed intense labeling of microtubules and fine ultrastructural preservation.

MATERIALS AND METHODS

Fixation and Dehydration. Cells of the *Potorous tridactylis* kidney cell line (Pt K1) and cells of the Madin–Darby canine kidney cell line (MDCK) were grown on coverslips and fixed at room temperature for 30 min with 1.0% glutaraldehyde (vol/vol) in 0.1 M Hepes, pH 7.2. They were then treated for 5 min in 0.1% Triton X-100 in 0.1 M Hepes, rinsed, and placed into $NaBH_4$ at 1 mg/ml H_2O for 30 min. Pieces of small intestine from newly hatched chicks were fixed for 90 min in 0.1% glutaraldehyde, 4.0% paraformaldehyde (wt/vol) in 0.1 M Hepes. Fertilized sea urchin eggs (*Strongylocentrotus purpuratus*) were fixed in 1.0% glutaraldehyde (vol/vol) in 0.4 M sodium acetate, 25 mM EGTA, 5 mM $MgCl_2$, pH 6.2. Cells or tissues were rinsed in the appropriate buffer, dehydrated through a graded acetone series, and placed in dichloromethane. Absolute acetone and dichloromethane were stored over molecular sieve.

Embedding, Sectioning, and Extraction. The embedding compound (EC) was prepared by dissolving 120 g of polymethylmethacrylate (Plexiglas, grade MC; Rohm and Haas) and 6 ml of dibutyl phthalate in 600 ml of dichloromethane. The compound was stable at least 1 year at room temperature. For infiltration cells or tissues were gently agitated in a 1:3 mixture of EC and dichloromethane for 1 hr in a 1:1 mixture for 2 to 4 hr, and in complete EC overnight. Samples were transferred to scintillation vial caps (25 mm in diameter and 12 mm high made of either polyethylene or polypropylene) and covered with EC to a depth of ≈5-fold the thickness of the sample. The caps were placed in the fume hood together in a glass Petri dish and loosely covered to maintain a high solvent–vapor concentration above the samples. This served to maintain the surface of the EC liquid during evaporation. After 8 to 12 hr the slightly soft plastic was pried from the caps and left uncovered in the fume hood for several more hours until the plastic was fully hardened. Embedded tissues were cut out with razor blades and glued to Epon blocks. Samples were sectioned 0.25- to 0.75-μm thick with glass knives onto water-filled troughs. Sections were collected on polylysine-coated coverslips for immunofluorescence or on Formvar/carbon-coated nickel grids for immunogold labeling.

Sections of tissue culture cells were dried down and the plastic was extracted by immersion of coverslips or grids in acetone for 10 min. For intestine and egg sections, better labeling was obtained when sections were left on small drops of water on coverslips. Before the sections had dried down the coverslips were carefully immersed in a 3:1 mixture of chloroform and acetone and then were incubated for 60 min until the plastic had dissolved, and the water had dispersed depositing the sections on the coverslips. After rinsing in acetone and ethanol the sectioned tissues were treated with $NaBH_4$ at 1.0 mg/ml ethanol overnight. The sections were rinsed in H_2O before immunolabeling.

Immunolabeling. Immunofluorescent labeling was per-

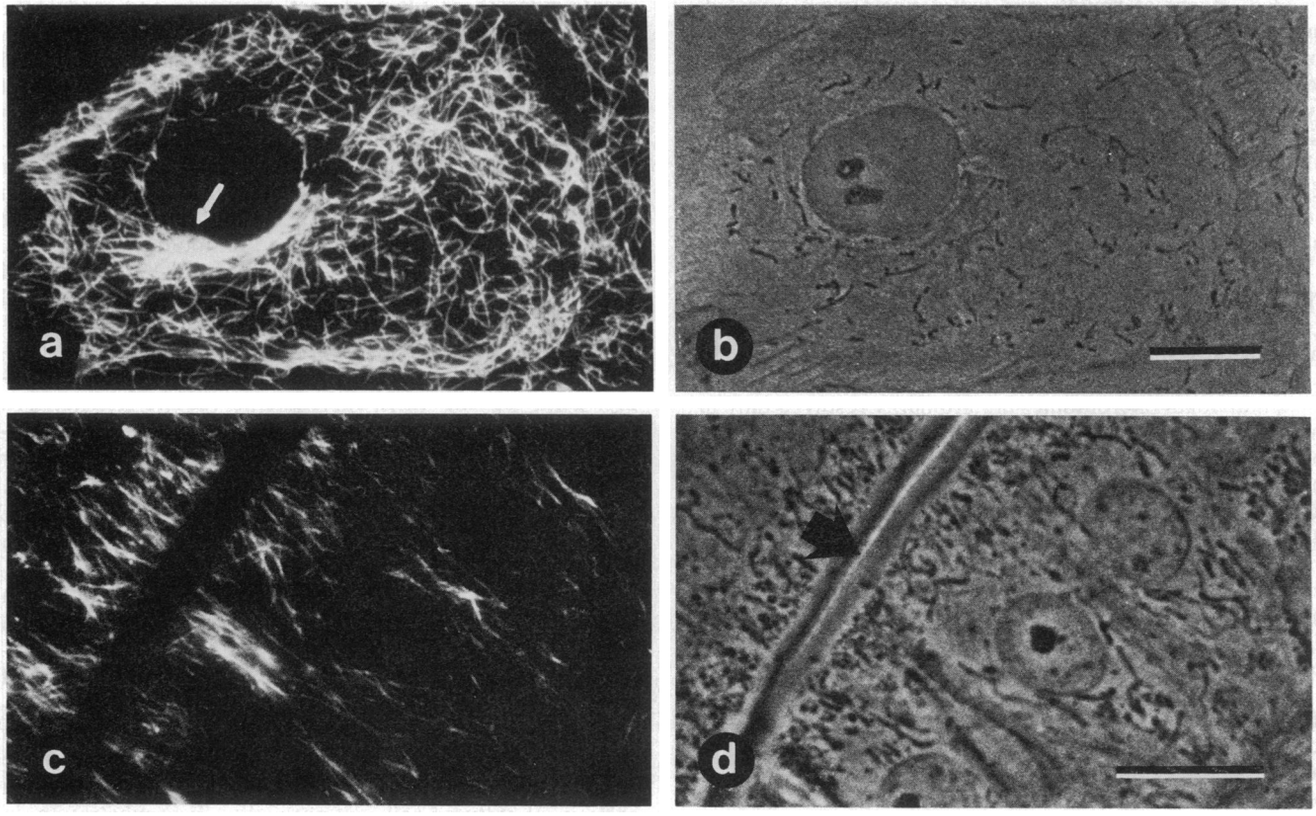

FIG. 1. Microtubule patterns in interphase cells and tissues. Indirect immunofluorescent (*a*) and phase-contrast (*b*) images of 0.5-μm sections of interphase Pt K1 cell immunolabeled for tubulin. Distinct labeled fibers course through the cytoplasm. Many are focused at the microtubule-organizing center (MTOC) (arrow). Very short labeled fibers are the result of microtubules that run only a brief distance in the plane of the section. Indirect immunofluorescent (*c*) and phase-contrast (*d*) images of 0.5-μm section of chick intestinal epithelium. Two rows of cells from adjacent villi are closely apposed but separated by a narrow gap (arrowhead) that is continuous with the intestinal lumen. Microtubules generally parallel the long axes of cells ending abruptly at the terminal web. The microtubules are apparently not focused at a MTOC. (Bars = 10 μm; *a* and *b*, ×1500; *c* and *d*, ×2000.)

formed by standard procedures (30) using a rat monoclonal anti-tubulin antibody (a gift from John Kilmartin, Medical Research Council, Cambridge, England) and a fluoresceinated goat anti-rat antibody (Cooper Biomedical, Malvern, PA). After labeling the coverslips were air-dried, mounted in 10% polyvinyl alcohol containing *p*-phenylenediamine at 1 mg/ml and observed with a Zeiss Universal microscope equipped with epifluorescence optics.

Sections on grids were labeled by the immunogold procedure of DeMey (31) except that incubation with the gold-conjugated secondary antibody was done for 6 to 8 hr. After labeling, grids were washed with water and postfixed with 0.1% osmium tetroxide, 1.0% uranyl acetate (wt/vol). Grids were rinsed in water, dehydrated in acetone, and dried by the critical point method incorporating the precautions advised by Ris (32). Samples were observed at 1 MV with an AEI-7 high-voltage electron microscope.

RESULTS

Typically, immunofluorescence images of cultured cells are obtained from whole mount preparations. In these preparations, microtubules can be identified as long fibers but they are clearly resolved only at the cell periphery (33). In the nuclear region, the cell thickness (5–10 μm) and the number of microtubules (upward of a hundred) have precluded the visualization of single fibers. Using the REC method, we visualized the microtubule network in sections of cultured interphase epithelial cells with indirect immunofluorescence (Fig. 1 *a* and *b*). Individual fibers, presumably single microtubules, were clearly resolved throughout the cytoplasm even near the cell nucleus. Some microtubules that extended only a brief distance in the plane of the section (0.5-μm thick) appeared as very short labeled fibers.

The REC method also permitted us to examine the microtubule network in epithelial cells in intact tissues. Fig. 1 *c* and *d* shows a section of chick intestinal epithelium decorated with anti-tubulin. Microtubules parallel the long axes of the cells and terminate abruptly at the terminal web. Unlike the cells in culture, the microtubule pattern in the epithelial cells in tissue is apparently not focused at a MTOC.

The mitotic pattern of microtubule organization was analyzed in a variety of cell types. The cultured cell line, MDCK (Fig. 2 *a* and *b*), was selected because it self-organizes *in vitro* into an epithelial colony exhibiting cell junctions and apical–basal polarity (34, 35). Again, the chick intestinal epithelium (Fig. 2*c*) was our example of an intact tissue, and the sea urchin egg (Fig. 2*d*) was used to test the method on a very large cell (75-μm diameter). In each instance, clear images of mitotic spindles showing astral and chromosomal fibers were obtained. The organization of the mitotic spindle in the cells of the intestinal epithelium was similar to that of mitotic MDCK cells. The REC method permitted us to track microtubule fibers from the aster of the sea urchin egg all the

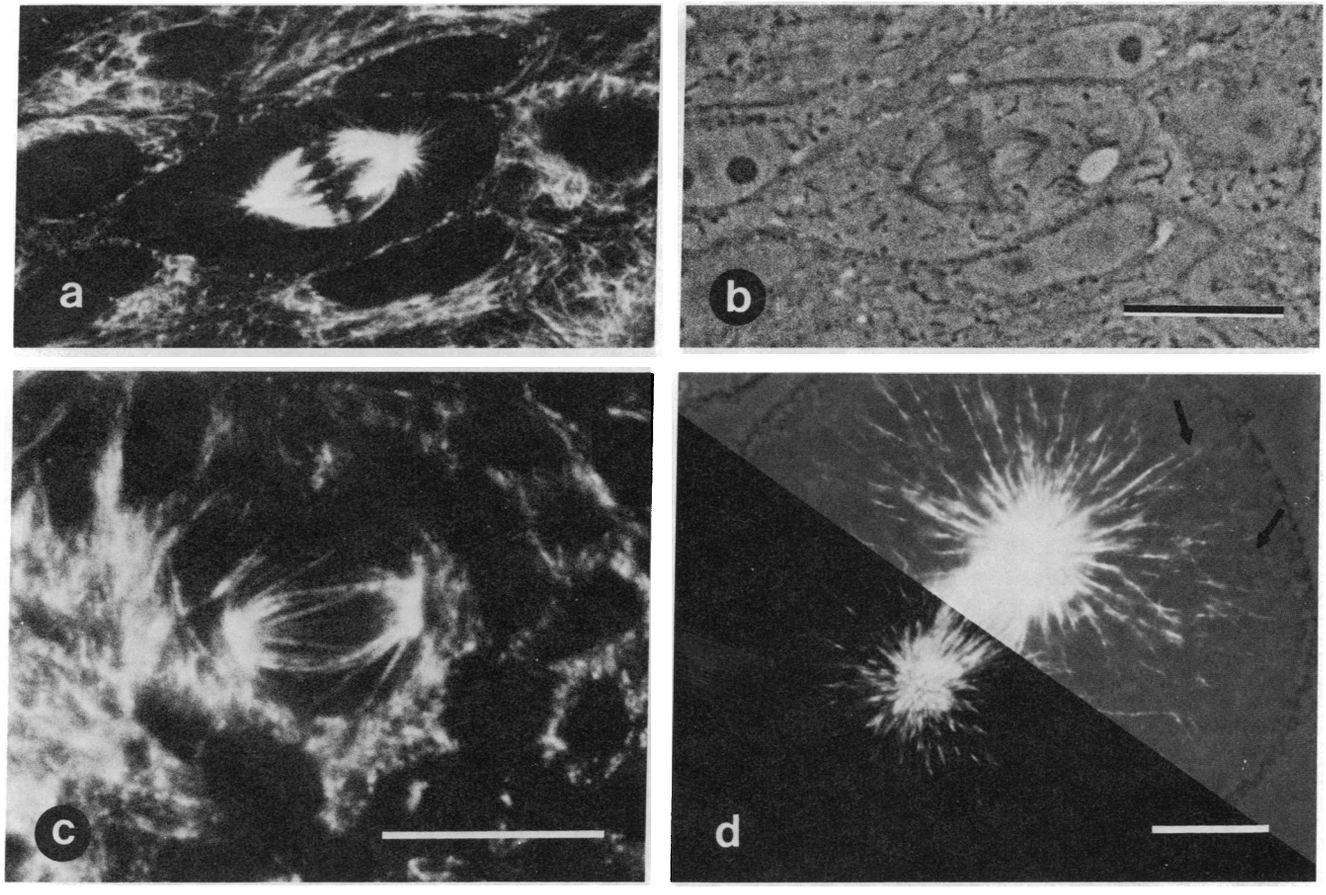

FIG. 2. Mitotic spindles in cells and tissues. Indirect immunofluorescent (*a*) and phase-contrast (*b*) images of a 0.5-μm section of a metaphase MDCK cell immunolabeled for tubulin. Spindle fiber bundles and astral fibers extending from the centrosomes are evident. (*c*) Indirect immunofluorescent image of a 0.75-μm section of an intestinal epithelial cell in late anaphase immunolabeled for tubulin. Long labeled fibers extend from pole to pole. (*d*) Combined immunofluorescent and phase-contrast images of a 0.75-μm section of a sea urchin egg in first-division anaphase. This photograph was printed using a darker fluorescent exposure for the lower half-spindle to highlight the spindle fibers and a lighter exposure for the upper half-spindle to better visualize the astral microtubules extending from the centrosome to the vicinity of the egg surface (arrows). The egg surface has been rendered visible in the photograph by superimposing the phase-contrast image of the section on the fluorescent image. (Bars = 10 μm; *a* and *b*, ×2200; *c*, ×3000; *d*, ×1600.)

way to the cell surface, an observation not previously possible with whole mount techniques (36).

At the electron microscopic level, sections of Pt K1 cells treated with anti-tubulin followed by a secondary antibody adsorbed to 20-nm colloidal gold particles revealed intensely labeled tracks of microtubules (Fig. 3). The fine structure of the unlabeled cytoskeletal filaments was well preserved. Since the embedding plastic is removed in the REC method, the contrast of cytoplasmic structures is greatly increased, facilitating observation of even relatively thick sections. While low contrast immunolabels such as ferritin-linked antibodies would be difficult to discern, 20-nm gold particles were easily visualized even at low electron microscopic magnification. Hence, both the overall pattern of labeled microtubules and the specific interactions of organelles with microtubules are available for study. In Fig. 3*b*, mitochondria are seen clearly associated with microtubules, and in Fig. 3*c*, the spindle and astral fibers of mitotic cells are heavily labeled, although the gold particles are packed too densely to track individual microtubules.

DISCUSSION

We have developed a post-embedding immunolabeling technique with increased resolution, range of applicability, and ease of use. No specialized equipment or skills are required. Unlike methods that utilize epoxy or other acrylic resins, REC involves no chemical polymerization and crosslinking. Thus, antigenicity of target molecules is maximized. The method is suitable for light microscopic immunofluorescence and electron microscopic immunolabeling and affords a high degree of structural preservation.

In whole mounts there is a contribution to background fluorescence from labeled microtubules above or below the

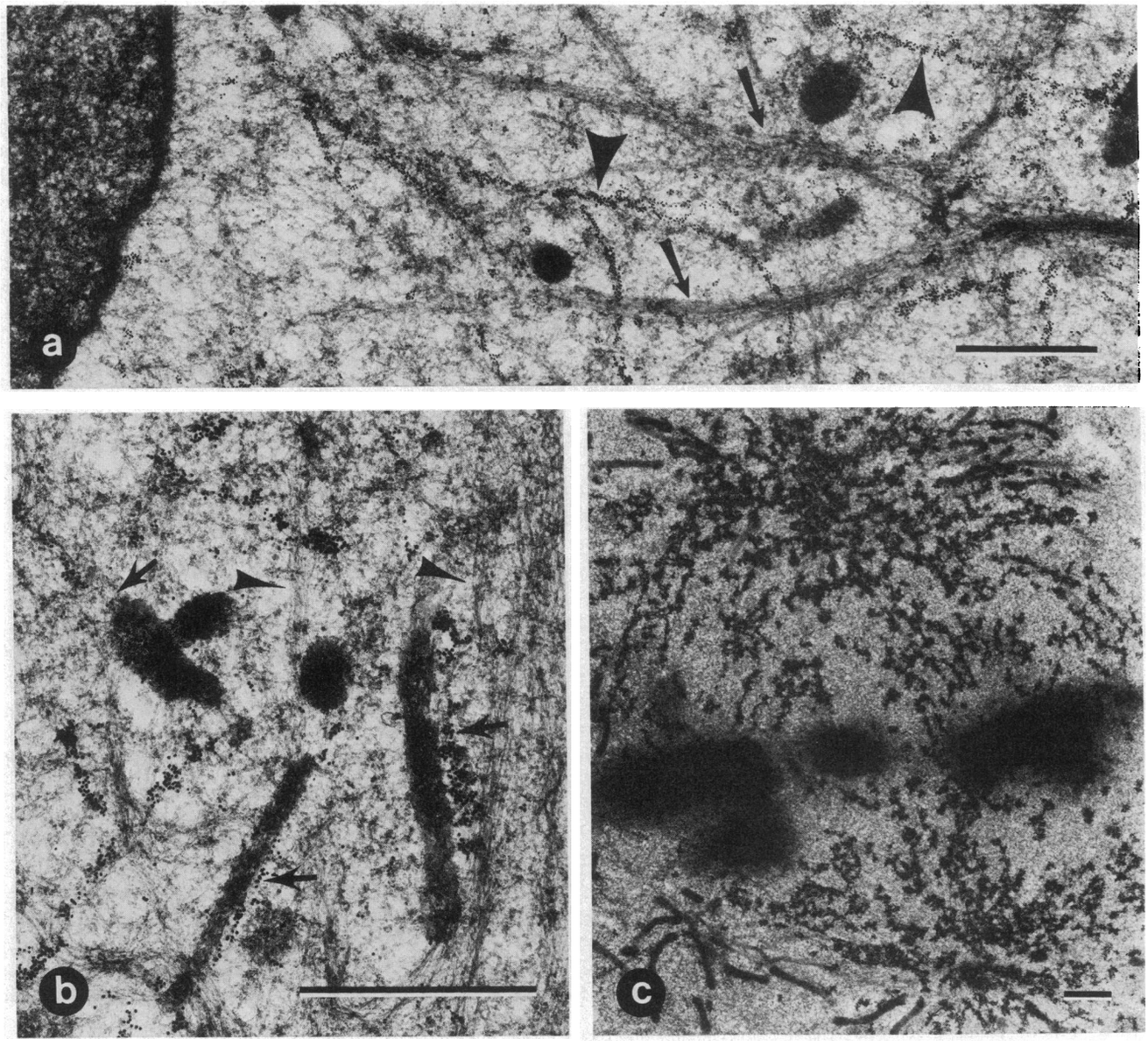

FIG. 3. High-voltage electron microscopic imaging of sections of Pt K1 cells immunolabeled with anti-tubulin antibody followed by secondary antibody adsorbed to 20-nm colloidal gold. (*a*) Low magnification survey view of cell sectioned at 0.5 μm. Densely labeled microtubules (arrowheads) course through the cytoplasm interspersed among a meshwork of fine cytoplasmic filaments and several bundles of intermediate filaments (arrows). (*b*) Higher magnification view of a 0.25-μm section showing lateral association of mitochondria (arrows) with labeled microtubules. Note the preservation of the unlabeled intermediate filaments (arrowheads). (*c*) A 0.5-μm section of a mitotic Pt K1 cell showing intense labeling of spindle and astral fibers. (Bars = 1.0 μm; *a*, × 22,000; *b*, ×37,000; *c*, ×7500.)

focal plane, except in very thin regions such as the periphery of cultured cells. With REC, since sections are observed, such background is eliminated. Thus, fine fibers such as the astral microtubules of the mitotic figures were clearly resolved. In addition, patterns of great complexity in whole mounts such as the microtubule network near the nuclei of cultured cells were more easily visualized through the use of labeled semi-thick sections. If desired, images from serial sections could be used to reconstruct the complete three-dimensional pattern of microtubules.

We found that the majority of microtubules in intact intestinal epithelium were parallel to the basal-apical axes of the cells and were not focused on a MTOC. This distribution is consistent with roles for the microtubules in maintaining the elongated profile of the cells and/or participating in intracellular transport of vesicles from the Golgi and between the apical and basolateral surfaces. The microtubule distribution seen *in vivo* was quite different from that observed in epithelial cell lines grown *in vitro*. In cultured cells, most microtubules were parallel to the substratum, and were focused toward a MTOC. In contrast, the mitotic spindles in cells of intact epithelium and in epithelial cell lines showed close structural similarity.

The microtubule network was examined at the electron microscopic level in cultured cells. In sections of Pt K1 cells we were able to view both the extended array of microtubules and examine specific microtubule interactions with mitochondria. Unlike many immunoelectron microscopic studies, where structural associations are dependent upon fortuitous inclusion of interacting elements in the same thin section, we could easily examine sections 0.25- or 0.5-μm thick. Thus far our immunoelectron microscopic studies have been restricted to cultured cells. Gold-labeled antibodies appear to penetrate more poorly into sections of intact tissues. Difficulties in obtaining complete penetration of antibodies into tissues have long plagued immunocytochemistry (2–5), and this problem has been noted by investigators using other reversible embedding methods for labeling sections (27).

Detailed descriptions of microtubule distributions in different stages of the cell cycle, in various differentiated cell types, in embryos, and in cells responding to a variety of experimental treatments are essential for understanding the functions of microtubules. REC should greatly facilitate these studies. In addition, it should be possible to test more adequately whether information from studies using cultured cells can be extrapolated to *in vivo* systems. Moreover, REC is a general technique that can be used to enhance access affinity labels including antibodies, lectins, and hybridization probes to cellular components. Thus, this method should find wide application in many studies. Other uses of the technique in areas such as direct ultrastructural imaging are presented elsewhere (37).

We thank Steven Limbach and Hsien-Ming Chu for technical assistance. This work is supported by Grants RR00570 to H. Ris and GM25062 to G.G.B. from the National Institutes of Health.

1. Rieder, C. L. & Bowser, S. S. (1985) *J. Histochem. Cytochem.* **33**, 165–171.
2. Piekut, D. T. & Casey, S. M. (1983) *J. Histochem. Cytochem.* **31**, 669–674.
3. Willingham, M. C., Yamada, S. S. & Pastan, I. (1978) *Proc. Natl. Acad. Sci. USA* **75**, 4359–4363.
4. Eldred, W. D., Zucker, C., Karten, H. J. & Yazulla, S. (1983) *J. Histochem. Cytochem.* **75**, 5511–5515.
5. Brown, W. J. & Farquhar, M. G. (1984) *Cell* **36**, 295–307.
6. Moriarty, G. C. & Halmi, N. S. (1972) *J. Histochem. Cytochem.* **20**, 590–603.
7. Parsons, J. A. & Erlandsen, S. L. (1974) *J. Histochem. Cytochem.* **22**, 340–351.
8. Roth, J., Bendayan, M. & Orci, L. (1978) *J. Histochem. Cytochem.* **26**, 1074–1081.
9. Knecht, E., Hernandez, J., Wallace, R. & Grisolia, S. (1979) *J. Histochem. Cytochem.* **27**, 975–981.
10. Bendayan, M., Roth, J., Perreht, A. & Orci, L. (1980) *J. Histochem. Cytochem.* **28**, 149–160.
11. Thomson, R. O., Walker, P. D., Batty, I. & Baillie, A. (1967) *Nature (London)* **215**, 393–394.
12. Kawarai, Y. & Nakane, P. K. (1970) *J. Histochem. Cytochem.* **18**, 161–166.
13. Shahrabadi, M. S. & Yamamoto, T. (1971) *J. Cell Biol.* **50**, 246–250.
14. Lundgren, B. & Westin, M. (1974) *J. Ultrastruct. Res.* **46**, 230–238.
15. Takamiya, H., Batiford, S. & Vogt, A. (1980) *J. Histochem. Cytochem.* **28**, 1041–1049.
16. Roth, J., Bendayan, M., Carlemalm, E. C., Villiger, W. & Garavito, M. (1981) *J. Histochem. Cytochem.* **29**, 663–671.
17. Newman, G. R., Jasani, B. & Williams, E. D. (1983) *Histochem. J.* **15**, 543–555.
18. Craig, S. & Miller, C. (1984) *Cell Biol. Int. Rep.* **8**, 879–886.
19. Bendayan, M. & Zollinger, M. (1983) *J. Histochem. Cytochem.* **31**, 101–109.
20. Painter, R. G., Tokuyasu, K. T. & Singer, S. J. (1973) *Proc. Natl. Acad. Sci. USA* **70**, 1649–1653.
21. Tokuyasu, K. T. (1980) *Histochem. J.* **12**, 381–403.
22. Pinto Da Silva, P., Kachar, B., Torrisi, M. R., Brown, C. & Parkison, C. (1981) *Science* **213**, 230–233.
23. Geuze, H. J., Slot, J. W., van der Lay, P. A. & Scheffer, R. C. T. (1981) *J. Cell Biol.* **89**, 653–665.
24. Griffiths, G., Brands, R., Burke, B., Louvard, D. & Warren, G. (1982) *J. Cell Biol.* **95**, 781–792.
25. Tokuyasu, K. T. (1983) *J. Cell Biol.* **97**, 562–565.
26. Slot, J. W. & Geuze, H. J. (1983) in *Immunohistochemistry*, ed. Cuello, A. C. (Wiley, New York), pp. 323–346.
27. Wolosewick, J. J. & DeMey, J. (1982) *Biol. Cell.* **44**, 82–88.
28. Wolosewick, J. J., DeMey, J. & Meininger, V. (1983) *Biol. Cell.* **49**, 219–226.
29. Parysek, L. M., Wolosewick, J. J. & Olmstead, J. B. (1984) *J. Cell Biol.* **99**, 2287–2296.
30. Weber, K., Bibring, T. & Osborn, M. (1975) *Exp. Cell Res.* **95**, 111–120.
31. DeMey, J. R. (1983) in *Immunohistochemistry*, ed. Cuello, A. C. (Wiley, New York), pp. 347–372.
32. Ris, H. (1984) *J. Cell Biol.* **100**, 1474–1487.
33. Weber, K. (1976) in *Cell Motility*, eds. Goldman, R., Pollard, T. & Rosenbaum, J. (Cold Spring Harbor Laboratory, Cold Spring Harbor, NY), Vol. A, pp. 403–417.
34. Misfeldt, D. S., Hamamoto, S. T. & Pitelka, D. R. (1976) *Proc. Natl. Acad. Sci. USA* **73**, 1212–1216.
35. Cereijido, M., Robbins, E. S., Dolan, W. J., Rotunno, C. A. & Sabatini, D. D. (1978) *J. Cell Biol.* **77**, 853–880.
36. Harris, P., Osborn, M. & Weber, K. (1980) *J. Cell Biol.* **84**, 668–679.
37. Gorbsky, G. & Borisy, G. G. (1985) *J. Histochem. Cytochem.*, in press.